Pitch and Roll Damping Coefficients of the Australian 81mm Improved Mortar Projectile

David A. Pierens

DEPARTMENT OF DEFENCE
DEFENCE SCIENCE AND TECHNOLOGY ORGANISATION

Pitch and Roll Damping Coefficients of the Australian 81mm Improved Mortar Projectile

David A. Pierens

Aeronautical and Maritime Research Laboratory

ABSTRACT

Technical Report

This report presents roll damping coefficients and pitch damping coefficients obtained from dynamic rolling tests and static wind tunnel tests of the Australian 81mm Improved Mortar Projectile, IMP. An 80% scale model was used in the dynamic roll tests and a full scale model was used in the static wind tunnel tests.

APPROVED FOR PUBLIC RELEASE

DSTO-TR-0020

DEPARTMENT OF DEFENCE

DEFENCE SCIENCE AND TECHNOLOGY ORGANISATION

Published by

DSTO Aeronautical and Maritime Research Laboratory
GPO Box 4331
Melbourne Victoria 3001 Australia

Telephone: (03) 626 7000
Fax: (03) 626 7999

AR No. 008-330
May 1994

APPROVED FOR PUBLIC RELEASE

CONTENTS

List of Figures

List of Tables

Nomenclature

C_l	rolling moment coefficient, torque coefficient
C_{l_o}	static rolling moment coefficient
C_{l_p}	roll damping coefficient
C_{m_q}	pitch damping coefficient
D	drag force
l	rolling moment
L	lift force
m	pitching moment
X	axial force
Z	normal force
θ	pitch angle (deg)

Force and Moment Axis System

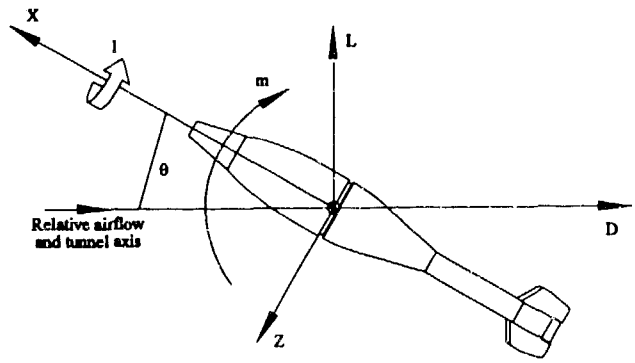

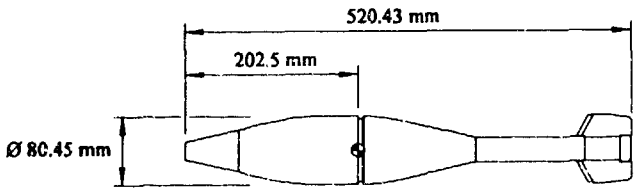

C.G. location on full scale projectile

1. Introduction

The Australian Army's Engineering Development Establishment (EDE) is working with Australian Defence Industries Pty Ltd (ADI) to develop and produce a new improved 81mm mortar projectile to replace the M374 High Explosive (HE) round. The Weapon Aerodynamics Discipline of the Aeronautical Research Laboratory (ARL) was requested by Explosive Ordnance Division (EOD) of Materials Research Laboratory (MRL) to determine pitch and roll damping data (C_{m_q} and C_{l_p} respectively) for the 81mm mortar from wind tunnel tests. The data will be added to existing static aerodynamic data obtained from previous wind tunnel tests of an 80% and 100% scale mortar model (references 1 and 2), and will be used to model the flight behaviour of the mortar and to establish its stability and range and the effect of launch transients.

2. Test Details

2.1 Wind Tunnel

The wind tunnel used for these tests was the ARL-Salisbury S1 wind tunnel which is a closed circuit continuous operation tunnel. The working section has dimensions of 380 mm x 360 mm with slots and has the capability for Mach numbers of 0.35 to 1.0 and 1.4 to 2.8. Tunnel flow conditions are set and recorded using a static pressure port upstream of the model, a pitot tube located upstream of the contraction, and a temperature probe in the settling chamber. The model was positioned in the working section by a pitch and roll mechanism located beneath the working section.

2.2 Models

Models tested were an 80% scale metal model and a full scale metal model. Both models were designed and manufactured at ARL, based on drawings of the full scale Improved Mortar Projectile (IMP) supplied by EDE and ADI. 80% scale and full scale HL 18622-022 fuzes and DE 132410018 (extruded, canted metal) fins were attached to the corresponding scale model.

2.3 Experimental Technique

2.3.1 Roll Damping

Roll damping coefficients, C_{l_p}, were obtained from dynamic wind tunnel tests carried out with an 80% mortar model attached to a roll balance as shown in figures 1 and 2.

The roll balance is fitted with a brake which consists of an expanding fibrous ring operated by compressed air working on pistons in the balance shaft. With the brake on, the wind tunnel was started, and once the desired Mach number was reached, the brake was released, allowing the model to accelerate from rest to a constant roll rate. During this time, roll rates and corresponding times were recorded and saved to disk. Tests were carried out at Mach numbers of 0.5, 0.7, 0.8, 0.9 and 0.95, which encompasses the flight speed range of the 81mm IMP mortar, at pitch angles of 0°, 5° and 10°.

Values of C_{l_p} were calculated from the dynamic rolling data, combined with static rolling moment data obtained from reference 1. A detailed description of the derivation is given in Appendix A.

2.3.2 Pitch Damping

Pitch damping coefficients were calculated using the technique given in reference 4. This uses static aerodynamic lift data for lifting surfaces and the body acting separately to determine the contribution of each to the overall pitch damping.

The fin lift characteristics were determined from wind tunnel tests on a full scale model. Tests were conducted at Mach numbers of 0.5, 0.7, 0.8, 0.9 and 0.95 and through a pitch angle range of -5° to +5°, first on the model with fins attached, and then with a plain cylindrical tail piece (no fins) attached. The difference between the "fins on" and the "fins off" lift curve slopes was taken to be the lift curve slope of the fins alone operating in the body wake. These tests were conducted as part of a larger test program, and are described in more detail in reference 2.

Appendix C describes the theoretically based derivation of the body lift contribution, and the use of the fin and body contributions to calculate the overall pitch damping coefficients.

3. Discussion of Results

3.1 Roll Damping

Values of C_{l_p}, derived from the method described in Appendix A, are presented in table 1 and plotted in figure 3.

Mach No.	Roll Damping Coefficient, C_{l_p}		
	$\alpha = 0°$	$\alpha = 5°$	$\alpha = 10°$
0.50	-0.245	-0.242	-0.256
0.70	-0.259	-0.256	-0.281
0.80	-0.268	-0.260	-0.302
0.90	-0.268	-0.270	-0.299
0.95	-0.300	-0.314	-0.347

Table 1: Roll damping coefficient, C_{l_p}

Estimates of the static rolling moment, C_{l_o}, can be obtained from the dynamic rolling moment data by extrapolating a least squares straight line fit to the data back to zero roll rate (see figure A3). The values of C_{l_o} so obtained differ from C_{l_o}'s reported in reference 1 by up to 10%. This gives a useful estimate of the uncertainty in using these data to calculate roll damping, therefore C_{l_p} values stated above should be regarding as having uncertainties of the order of ±10%.

3.2 Pitch Damping

Values of C_{m_q} derived from the method described in Appendix C are presented in table 2 and plotted in figure 4.

Mach No.	C_{m_q}
0.50	-32.4
0.70	-39.7
0.80	-41.4
0.90	-49.3
0.95	-49.4

Table 2: Pitch damping coefficient, C_{m_q}

Figure 4 also shows values of C_{m_q} for an M374 81mm mortar projectile taken from reference 3. Although this is a different projectile shape, the similarities are sufficient to expect the values of C_{m_q} to be similar. Comparison of the two sets of data shows that for Mach numbers up to 0.8, reasonable similarity is observed, but differences of practical importance exist at the higher Mach numbers. The divergence of results above Mach 0.8 may be due to the unusually large model size, resulting in significant wind tunnel wall interference effects at the higher Mach numbers. Reference 2 discusses this in more detail. Because of these effects, and the uncertainties inherent in the application of static data to the estimation of dynamic parameters, the pitch damping results presented here are estimated to have uncertainties of up to ±20%. However, for a fin-stabilised ballistic projectile of this type, this level of uncertainty is acceptable in terms of predicting the overall flight trajectory.

4. Conclusion

Roll damping coefficients obtained from dynamic wind tunnel tests at various Mach numbers and pitch angles are presented in table 1 and figure 3. These data are estimated to contain uncertainties of ±10% due to a lack of low roll rate data, and uncertainties in the measurement of roll bearing friction.

Values for pitch damping coefficient obtained using the theory presented in Appendix C (as obtained from reference 4) and static wind tunnel results, are presented in table 2 and figure 4. These data are estimated to contain uncertainties of up to ±20% due to wind tunnel wall interference and uncertainties inherent in the method. However, from comparison with other experiments, it appears that the theory presented in Appendix C produces acceptable approximations for pitch damping coefficients for configurations and conditions considered here.

References

1. **Walter, S.R.**, *Wind Tunnel Testing of the 81mm Improved Mortar Projectile*, ARL-FLIGHT-MECH-TM-430, October 1991.

2. **Pierens, D.A.**, *Aerodynamic Evaluation of Production Fuzes and Fins for the 81mm Improved Mortar Projectile*, AR-008-331 (document in preparation).

3. **Rhodes, P.**, *An Aerodynamic and Stability Assessment of the 81mm Mortar Bomb fitted with the M734 Fuze*, TP 27298, Hunting Engineering Limited, UK, August 1984.

4. **ESDU Aerodynamics Sub-series Vol 9a Data Item 90010**, *Pitching Moment and Lift Force Derivatives Due to Rate of Pitch for Aircraft at Subsonic Speeds*, July 1990.

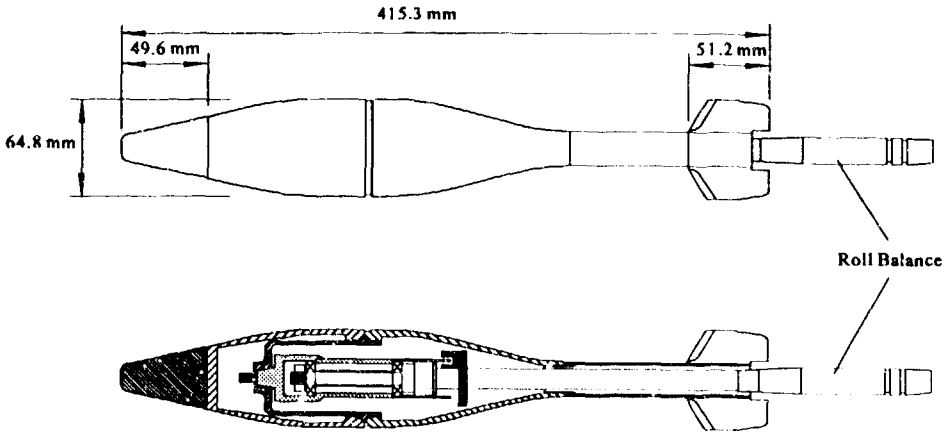

Figure 1: 80% 81mm mortar model and roll balance

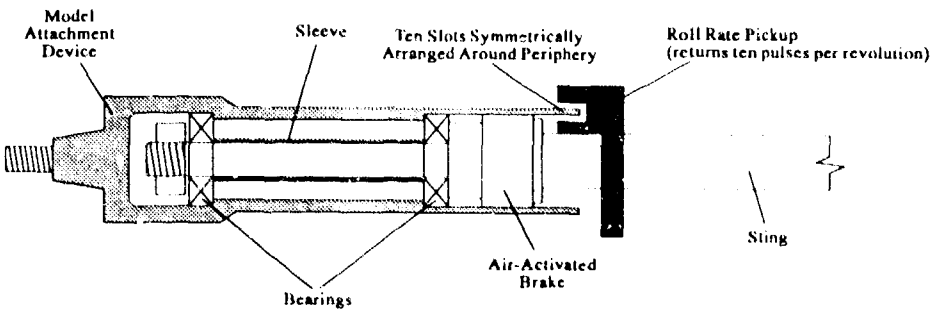

Figure 2. Roll balance

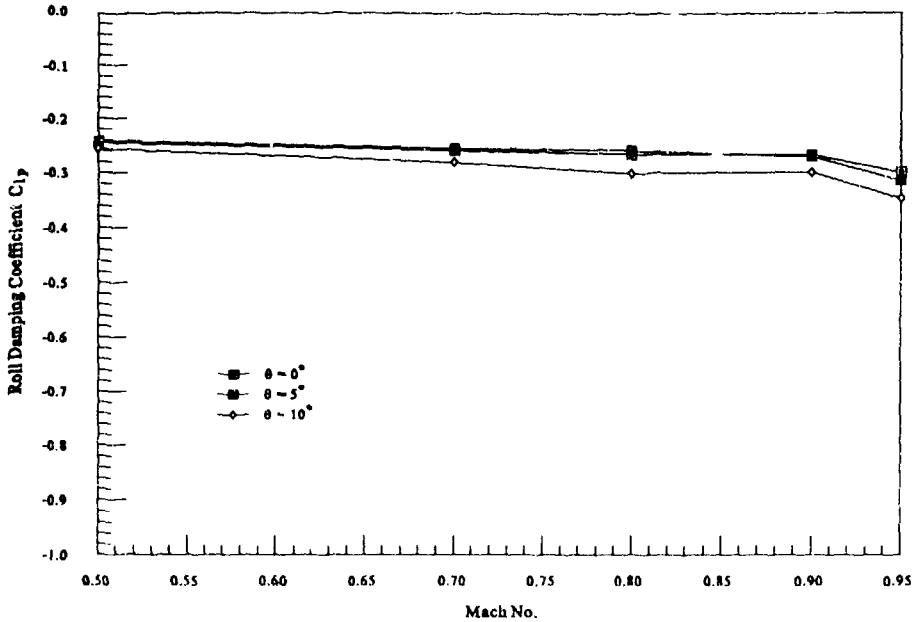

Figure 3: Roll damping coefficient, C_{l_p}, vs Mach No.

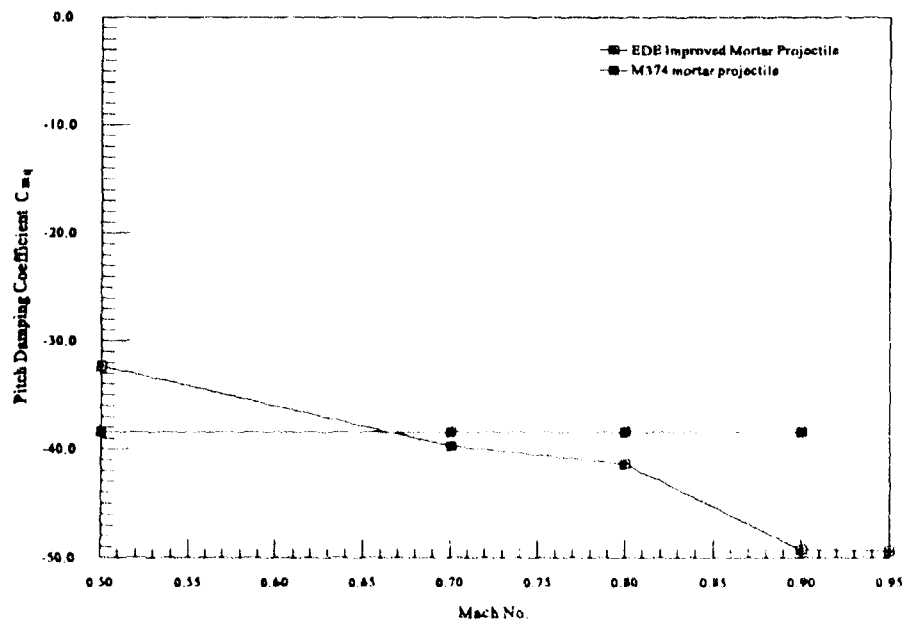

Figure 4: Pitch damping coefficient, C_{m_q}, vs Mach No.

APPENDIX A

DERIVATION OF C_{l_p}

Derivation of C_{l_p}

Symbols used:

C_l	rolling moment coefficient
C_{l_o}	static rolling moment coefficient
C_{l_p}	roll damping coefficient
d	reference length (diameter)
p	roll rate
V	velocity

The data for roll rate versus time (see figure A1 for an example of the roll rates obtained), were differentiated to produce values for roll acceleration versus time. From a knowledge of the roll inertia of the model, roll accelerations were then converted to roll torques, to give a set of roll torques versus roll rate. Bearing friction torque, as calculated in Appendix B, was then subtracted from the roll torque, producing values for aerodynamic torque versus roll rate. The aerodynamic torque was non-dimensionalised to obtain rolling moment coefficients, C_l, versus roll rate.

Roll damping coefficient, C_{l_p} was calculated using the following equation:

$$C_{l_p} = \frac{\delta C_l}{\delta p}\left(\frac{2V}{d}\right).$$

Due to the model's rapid acceleration, and the timebase on the Hewlett Packard digital oscilloscope used to record the data having to be set so as to cater for the high roll rates expected, roll rates less than 150 rad/s (≈ 24 Hz) could not be recorded. Due to the lack of low roll rate data, it was decided to include zero roll rate data (static rolling moment coefficients) measured in earlier tests and reported in reference 1. These data did not agree well with simple extrapolation of the dynamic data (see figure A3), throwing some doubt on the intermediate roll rate data. To get the best estimate of C_{l_p} it was decided to use only the two most reliable C_l values, ie. C_{l_o} from static test data and C_l at the maximum (constant) roll rate. Figure A2 shows the straight line drawn for Mach 0.95 using only these two extreme values. The gradient of this line is the roll damping coefficient, C_{l_p}, for Mach 0.95. C_{l_p} values for all other Mach numbers were obtained from the same procedure.

Note that, in figure A2 the magnitude of the bearing friction relative to the aerodynamic torque is indicated by the height above the roll rate axis at which maximum roll rate occurs. At this steady state roll rate, bearing friction equals aerodynamic torque. It can be seen that maximum bearing friction is about 5% of maximum aerodynamic torque, and hence moderate uncertainties in the measurement of bearing friction are not a significant contributor to the overall uncertainty of the result.

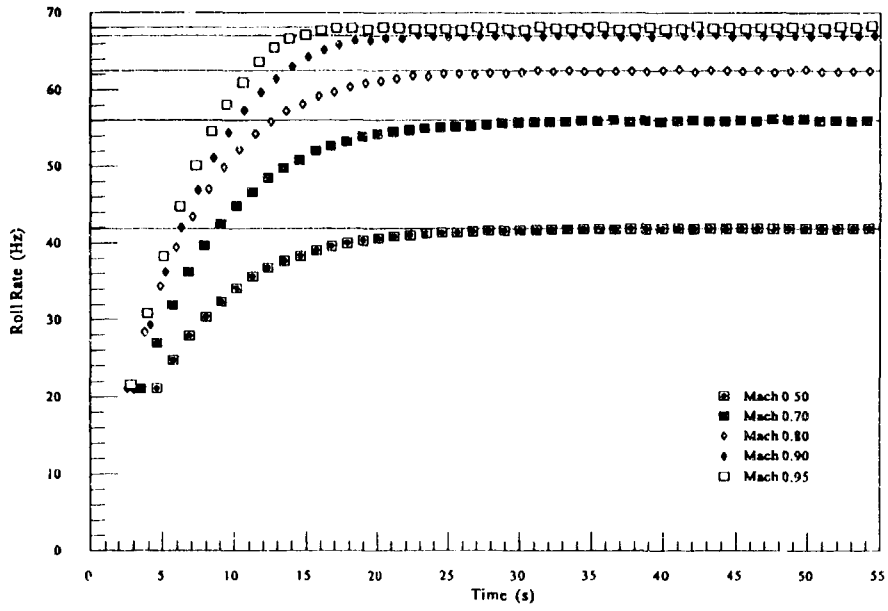

Figure A1: Roll rate vs time (for pitch angle = 0°)

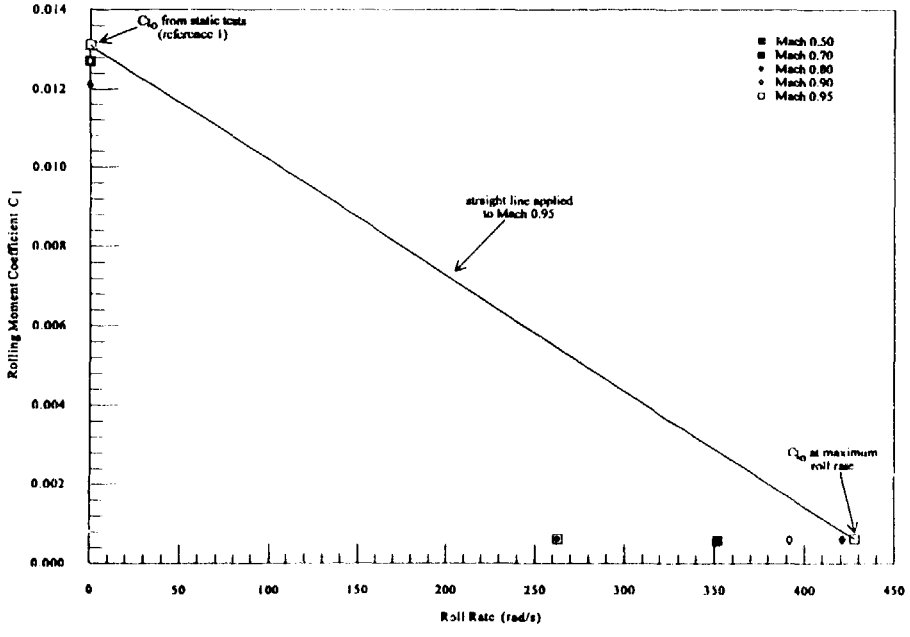

Figure A2: Rolling moment coefficient vs roll rate (for pitch angle = 0°)

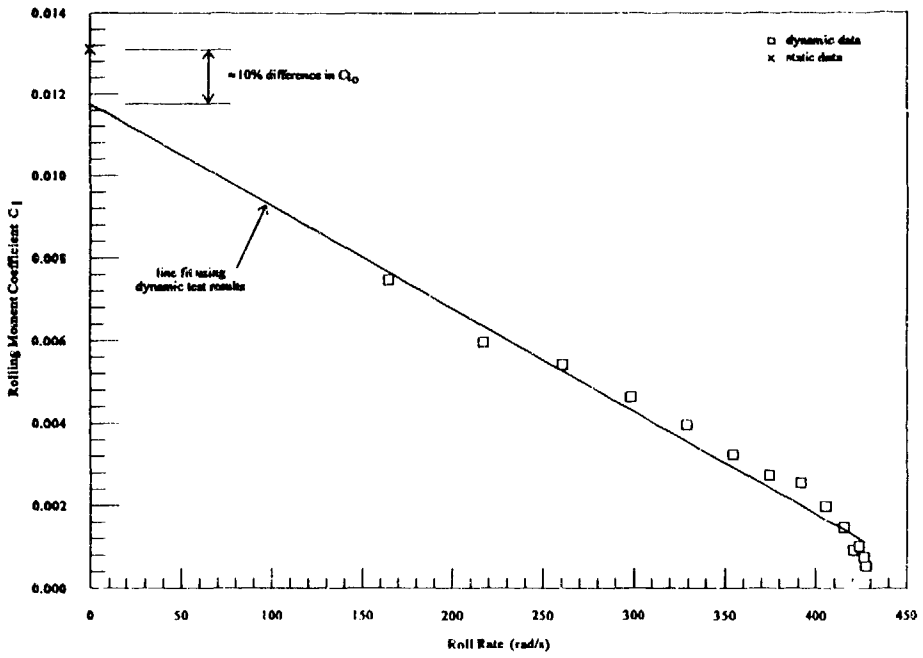

Figure A3: Comparison of C_{l_0} for Mach 0.95 and pitch angle = 0°

APPENDIX B

DETERMINATION OF ROLL BALANCE BEARING FRICTION

Determination of Roll Balance Bearing Friction

The model was removed from the balance and replaced with a simple flywheel. Compressed air from an air hose was then used to spin the balance with the flywheel attached. Once the balance had reached a roll rate slightly greater than the maximum constant spin rate observed during the wind tunnel tests, the air hose was removed and the balance allowed to come to rest. During this time, roll rate data were recorded and saved to disk. A Hewlett Packard digital oscilloscope was initially set to record the expected high roll rates, and when the roll rate reached the lower end of the timebase range, the timebase was changed so that the lower roll rates could be recorded. This procedure was carried out several times and all results were combined into one file.

The data for roll rate versus time were differentiated to produce values for roll acceleration versus time. From a knowledge of the inertia of the rotating parts, roll accelerations were then converted to bearing friction torques, to give a set of bearing friction torques versus roll rate. The graph of bearing friction torque versus roll rate is presented in figure B1 and has been approximated in further calculations by the two-segmented straight line fit shown there.

This method of measuring bearing friction neglects some parameters (eg. effects of variations in axial and radial loads). In this use, however, the aerodynamic and gravity loads on the bearings are only a very small fraction of the bearing design loads, and so are assumed to have a relatively small effect on the bearing friction characteristics. Also, bearing friction generally accounts for only a small part of the calculated roll damping (in this case, less than 5%) so that moderate uncertainties in the measurement of the bearing friction are not a significant contributor to the overall uncertainty of the roll damping measurements.

In a previous use of this technique, test runs were conducted in an evacuated chamber (S1 wind tunnel working section) to assess the contribution of aerodynamic damping. In these tests aerodynamic damping of the flywheel was found to be negligible compared to bearing friction.

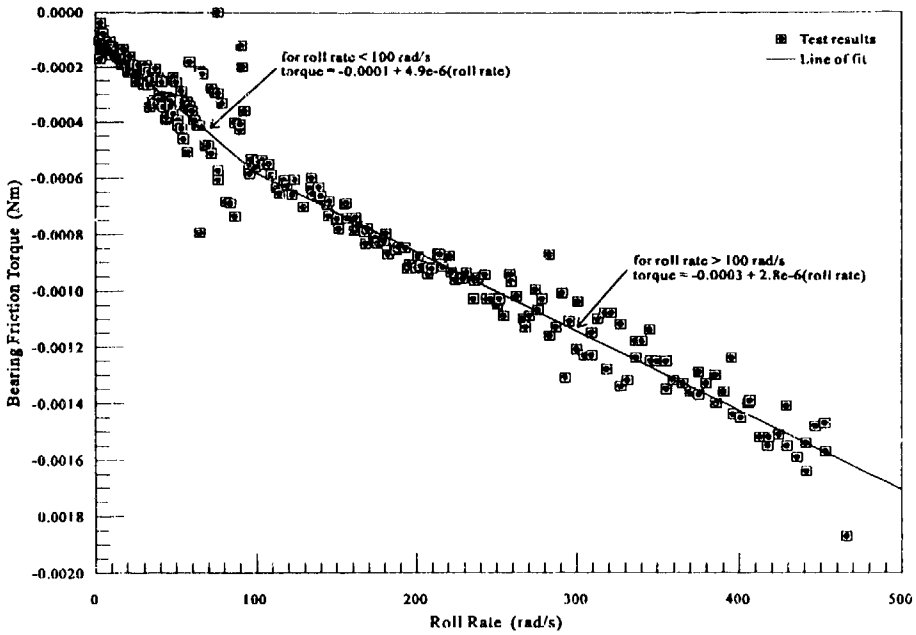

Figure B1: Bearing friction torque of roll damping rig

APPENDIX C

DERIVATION OF C_{m_q}

Derivation of C_{m_q}

The following derivation was obtained and modified from reference 4.

Notation:

a_{1F}	experimental lift curve slope of fin
C_{m_q}	pitch damping coefficient
$\bar{\bar{c}}$	reference length
d	mortar diameter
i	integer involved in summation to replace integral for $(M_q)_B$
k_a	parameter in calculation of afterbody correction factor $(1 - k_a)$
k_f	correction factor for body fineness
l_B	body length
l_o	distance of moment reference point aft of body nose
M	Pitching moment about moment reference point
$(M_q)_B$	body contribution to total pitching moment derivative
$(M_q)_F$	fin contribution to total pitching moment derivative
q	rate of pitch about moment reference point, positive nose up
S_B	planform area of body
S_m	cross-sectional area of body that contains maximum body width
S_w	reference length (cross-sectional area of mortar at maximum body width)
V_e	velocity of mortar relative to air in undisturbed flight
w_B	local body width
x_B	longitudinal distance along body axis to general body station, measured positive aft of moment reference point
x_F	longitudinal distance along body axis of ¼ chord point of aerodynamic mean chord of fin, measured positive aft of moment reference point
ρ	density of air

In reference 4 the pitch damping coefficient, C_{m_q}, is defined as

$$C_{m_q} = \frac{\delta M/\delta q}{\frac{1}{2}\rho V_e S_w \bar{\bar{c}}^2}$$

This equates to the definition of pitch damping, $C_{m_q} = \frac{\delta C_m}{\delta q}\left(\frac{2V}{d}\right)$, which is commonly used in missile work, where two different reference lengths are used, namely;

$\bar{\bar{c}} = d$ (missile diameter) for non-dimensionalising the pitching moments

and $\bar{\bar{c}} = \frac{d}{2}$ (missile radius) for non-dimensionalising the pitch damping coefficient.

$$C_{m_q} = \frac{\delta M/\delta q}{\tfrac{1}{2}\,\rho\, V_e\, S_w\,(d^2/2)} = 2\left(\frac{\delta M/\delta q}{\tfrac{1}{2}\,\rho\, V_e\, S_w\, d^2}\right) .$$

C_{m_q} is calculated as the sum of two contributions, namely body and fin, ie

$$C_{m_q} = (M_q)_B + (M_q)_F .$$

Body contribution, $(M_q)_B$ is calculated from

$$(M_q)_B = -\left(\frac{2\,S_m}{S_B}\right)\frac{k_f\,(1-k_a)}{S_w\,(d^2/2)} \int_{-l_o}^{l_B-l_o} w_B\, x_B^2\, dx_B .$$

To perform the integral in the equation above, the body was divided into twenty transverse segments of length $l_B/20$; these are numbered i = 1 to 20, from fore to aft. The local body width w_{Bi} and the local moment arm x_{Bi} are determined at the midpoint of each segment. The integral may then be approximated as

$$\int_{-l_o}^{l_B-l_o} w_B\, x_B^2\, dx_B \approx \left(\sum_{i=1}^{20} w_{Bi}\, x_{Bi}^2\right)\left(\frac{l_B}{20}\right) .$$

Fin contribution, $(M_q)_F$ is calculated from

$$(M_q)_F = -a_{1F}\frac{x_F}{d/2} ,$$

where a_{1F} (in this case) comes from wind tunnel measured data.

Calculated pitch damping coefficients at various Mach numbers are presented in the table below.

Mach No.	$(M_q)_B$	$(M_q)_F$	C_{m_q}
0.5	-5.760	-26.590	-32.350
0.7	-5.926	-33.808	-39.734
0.8	-6.040	-35.314	-41.354
0.9	-6.154	-43.096	-49.250
0.95	-6.230	-43.136	-49.366

Table C1: Pitch damping coefficients

As seen in table C1, the body contribution is relatively small (≈15% of the total). Therefore the uncertainty in the estimated C_{m_q} depends largely on the quality of the tail lift data. Being experimentally measured, this should be reliable.

DISTRIBUTION

DSTO-TR-0020

AUSTRALIA

DEFENCE ORGANISATION

Defence Science and Technology Organisation

Chief Defence Scientist
FAS Science Policy
AS Science Corporate Management
} shared copy
Counsellor Defence Science, London (Doc Data Sheet only)
Counsellor Defence Science, Washington (Doc Data Sheet only)
Senior Defence Scientific Adviser (Doc Data Sheet only)
Scientific Advisor Policy and Command (Doc Data Sheet only)
Navy Scientific Adviser (3 copies Doc Data Sheet only)
Scientific Adviser - Army
Air Force Scientific Adviser (Doc Data Sheet only)

Aeronautical and Maritime Research Laboratory
Director
Library Fishermens Bend
Chief Air Operations Division
Research Leader Aerodynamics
Chief Exposives Ordnance Division
Head Ordnance Systems
L. Krishnamoorthy

Electronics and Surveillance Research Laboratory
Director
Chief Guided Weapons Division
Research Leader Guided Weapons
Head Weapon Aerodynamics & Separation
Author: David A. Pierens
WAS File
Main Library - DSTO Salisbury

Defence Central

OIC TRS, Defence Central Library
Document Exchange Centre, DSTIC (8 copies)
Defence Intelligence Organisation
Library, Defence Signals Directorate (Doc Data Sheet Only)

Army

DWVP-A
Director Infantry
Infantry Centre Singleton
Engineering Development Establishment Library

OTHER ORGANISATIONS

Australian Defence Industries, St Marys

SPARES (6 COPIES)

TOTAL (37 COPIES)

AL 149 DEPARTMENT OF DEFENCE

PAGE CLASSIFICATION
UNCLASSIFIED

PRIVACY MARKING

DOCUMENT CONTROL DATA

1a. AR NUMBER	1b. ESTABLISHMENT NUMBER	2. DOCUMENT DATE	3 TASK NUMBER
AR-008-330	DSTO-TR-0020	MAY 1994	70/999

4. TITLE

PITCH AND ROLL DAMPING COEFFICIENTS OF AUSTRALIAN 81mm IMPROVED MORTAR PROJECTILE

5. SECURITY CLASSIFICATION (PLACE APPROPRIATE CLASSIFICATION IN BOX(S) IE. SECRET (S), CONF. (C) RESTRICTED (R), LIMITED (L), UNCLASSIFIED (U)).

DOCUMENT	TITLE	ABSTRACT
U	U	U

6. NO. PAGES: 24

7. NO. REFS.: 4

8. AUTHOR(S)

David A. Pierens

9. DOWNGRADING/DELIMITING INSTRUCTIONS

Not applicable.

10. CORPORATE AUTHOR AND ADDRESS

AERONAUTICAL AND MARITIME RESEARCH LABORATORY
AIR OPERATIONS DIVISION
GPO BOX 4331
MELBOURNE 3001

11. OFFICE/POSITION RESPONSIBLE FOR:

SPONSOR ARMY

SECURITY -

DOWNGRADING -

APPROVAL CAOD

12. SECONDARY DISTRIBUTION (OF THIS DOCUMENT)

Approved for public release.

OVERSEAS ENQUIRIES OUTSIDE STATED LIMITATIONS SHOULD BE REFERRED THROUGH DSTIC, ADMINISTRATIVE SERVICES BRANCH, DEPARTMENT OF DEFENCE, ANZAC PARK WEST OFFICES, ACT 2601

13a THIS DOCUMENT MAY BE ANNOUNCED IN CATALOGUES AND AWARENESS SERVICES AVAILABLE TO ...

No limitations.

14. DESCRIPTORS

Mortar
Roll damping
Pitch damping
Wind tunnel tests

15. DISCAT SUBJECT CATEGORIES

1902
0101

16. ABSTRACT

This report presents roll damping coefficients and pitch damping coefficients obtained from dynamic rolling tests and static wind tunnel tests of the Australian 81mm Improved Mortar Projectile, IMP. An 80% scale model was used in the dynamic roll tests and a full scale model was used in the static wind tunnel tests.

PAGE CLASSIFICATION
UNCLASSIFIED
PRIVACY MARKING

THIS PAGE IS TO BE USED TO RECORD INFORMATION WHICH IS REQUIRED BY THE ESTABLISHMENT FOR ITS OWN USE BUT WHICH WILL NOT BE ADDED TO THE DISTIS DATA UNLESS SPECIFICALLY REQUESTED.

16. ABSTRACT (CONT).

17. IMPRINT

AERONAUTICAL AND MARITIME RESEARCH LABORATORY, MELBOURNE

18. DOCUMENT SERIES AND NUMBER	19. WA NUMBER	20. TYPE OF REPORT AND PERIOD COVERED
Technical Report 0020	76 906J	

21. COMPUTER PROGRAMS USED

22. ESTABLISHMENT FILE REF (S)

M1/8/809

23. ADDITIONAL INFORMATION (AS REQUIRED)